Chinese Journal of Natural Medicines

Astragalus polysaccharide ameliorates ischemic stroke *via* modulating the microbiota–gut–brain axis

Yu Li, Jing Zhang, Shuo Li, Rui Zhu, Feifei Ou, He Xu, Yanan Wang, Yu Liu, Shihuan Tang, Jing Xu

Citation: Yu Li, Jing Zhang, Shuo Li, Rui Zhu, Feifei Ou, He Xu, Yanan Wang, Yu Liu, Shihuan Tang, Jing Xu, Astragalus polysaccharide ameliorates ischemic stroke *via* modulating the microbiota–gut–brain axis, Chinese Journal of Natural Medicines, 2026, 24(9), 1081–1093. doi: 10.1016/S1875–5364(26)61206–X.

View online: https://doi.org/10.1016/S1875–5364(26)61206–X

Related articles that may interest you

Xinglou Chengqi Decoction improves neurological function in experimental stroke mice as evidenced by gut microbiota analysis and network pharmacology

Chinese Journal of Natural Medicines. 2021, 19(12), 881–899 https://doi.org/10.1016/S1875–5364(21)60079–1

Tripterygium hypoglaucum extract ameliorates adjuvant–induced arthritis in mice through the gut microbiota

Chinese Journal of Natural Medicines. 2023, 21(10), 730–744 https://doi.org/10.1016/S1875–5364(23)60466–2

Guijiajiao (Colla Carapacis et Plastri, CCP) prevents male infertility *via* gut microbiota modulation

Chinese Journal of Natural Medicines. 2023, 21(6), 403–410 https://doi.org/10.1016/S1875–5364(23)60471–6

Danshen–Chuanxiongqin Injection attenuates cerebral ischemic stroke by inhibiting neuroinflammation *via* the TLR2/ TLR4–MyD88–NF– κ B Pathway in tMCAO mice

Chinese Journal of Natural Medicines. 2021, 19(10), 772–783 https://doi.org/10.1016/S1875–5364(21)60083–3

Biotransformation differences of ginsenoside compound K mediated by the gut microbiota from diabetic patients and healthy subjects

Chinese Journal of Natural Medicines. 2023, 21(10), 723–729 https://doi.org/10.1016/S1875–5364(23)60402–9

Chang Wei Qing Decoction enhances the anti–tumor effect of PD–1 inhibitor therapy by regulating the immune microenvironment and gut microbiota in colorectal cancer

Chinese Journal of Natural Medicines. 2023, 21(5), 333–345 https://doi.org/10.1016/S1875–5364(23)60451–0

Wechat

Chinese Journal of Natural Medicines 24 (2026) 1081-1093

Contents lists available at ScienceDirect

Chinese Journal of Natural Medicines

journal homepage: www.cjnmcpu.com/

Original article

Astragalus polysaccharide ameliorates ischemic stroke *via* modulating the microbiota-gut-brain axis

Yu Li[a,b], Jing Zhang[a,b], Shuo Li[c], Rui Zhu[c], Feifei Ou[a,b], He Xu[a,b], Yanan Wang[a,b], Yu Liu[c,*], Shihuan Tang[a,b,*], Jing Xu[a,b,*]

[a] *State Key Laboratory for Quality Essurance and Sustainable Use of Dao-di Herbs, Institute of Chinese Materia Medica, China Academy of Chinese Medical Sciences, Beijing 100700, China*

[b] *Institute of Chinese Materia Medica, China Academy of Chinese Medical Sciences, Beijing 100700, China*

[c] *Dongzhimen Hospital, Beijing University of Chinese Medicine, Beijing 100700, China*

ARTICLE INFO

Article history:
Received 21 January 2026
Revised 13 May 2026
Accepted 19 May 2026
Available online 20 September 2026

Keywords:
Ischemic stroke
Astragalus polysaccharide
Gut microbiota
LPS-TLR4-MAPK pathway
Microbiota-gut-brain axis

ABSTRACT

Ischemic stroke (IS) remains a major contributor to global disability and mortality. Astragalus polysaccharide (ASP), a naturally active component derived from *Astragalus membranaceus*, exhibits therapeutic potential against IS. However, their mechanism against IS *via* the microbiota-gut-brain axis remains unclear. Our study aimed to evaluate the mechanism of ASP against IS by middle cerebral artery occlusion (MCAO)-induced animal models combined with antibiotics (ABX) and fecal microbiota transplantation (FMT) experiments. In MCAO mice, our results showed that ASP significantly attenuated brain injury and intestinal barrier dysfunction. Transcriptomics, network pharmacology, and western blot identified LPS-TLR4-MAPK pathway as a key regulatory pathway in the regulation of IS-induced intestinal barrier dysfunction by ASP. Metagenomics and metabolomics indicated that ASP modulates SCFA-producing and anti-inflammatory bacterial genera (*g_Anaerobutyricum* and *g_Caproiciproducens*). Critically, ABX and FMT experiments confirmed that ASP's neuroprotective effects in MCAO mice receiving gut microbiota from IS patients, with this therapeutic benefit being microbiota-dependent. Additionally, LPS levels were upregulated in clinical patients with IS. In conclusion, our findings indicated that ASP alleviates IS-induced brain injury *via* the microbiota-gut-brain axis.

1. Introduction

Ischemic stroke (IS) is caused by an interruption of cerebral blood flow, which initiates a complex cascade of pathological events [1]. IS triggers disruption of the integrity of the blood-brain barrier (BBB), neuron loss, glial cell activation, and excessive inflammatory cytokines and free radicals release [2]. In addition to direct cerebral damage, IS triggers systemic responses through intricate neurohumoral pathways, resulting in damage to multiple peripheral organs, including the lungs, heart, kidneys, and gastrointestinal tract. These secondary injuries exacerbate the initial insult, ultimately contributing to severe and persistent neurological deficits [3]. Clinical evidence indicates that IS-induced intestinal barrier disruption rapidly triggers systemic inflammation through the excessive release of lipopolysaccharide (LPS), which further exacerbates brain injury. Consequently, therapeutic strategies targeting post-stroke intestinal protection may represent a crucial intervention point for improving outcomes in IS [4]. Current clinical management of IS primarily relies on acute interventions such as thrombolytic therapy, antiplatelet therapy, and mechanical thrombectomy [5]. While partially restoring cerebral blood flow, these approaches often fail to prevent secondary multi-organ damage. Consequently, many patients experience sequelae, including cognitive decline, limb paralysis, aphasia, and long-term organ dysfunction [6]. Therefore, elucidating the mechanisms underlying IS-induced brain and other organ injury and developing targeted neuroprotective and multi-organ therapeutic strategies are critical to improving long-term patient outcomes.

The growing evidence suggests that gut microbiota influences IS progression through the gut-brain axis. Following IS, the host disrupts intestinal homeostasis through multiple mechanisms, including stress response activation, systemic inflammatory cascades, and autonomic nervous system dysfunction, ultimately leading to intestinal dysfunction. This pathological manifestation is primarily characterized by a damaged intestinal barrier, altered microbial-derived metabolites, and gut microbiota dysbiosis. Notably, the intestinal flora imbalance promotes the overgrowth of Gram-negative bacteria, which depletes short-chain fatty acids (SCFAs) while increasing LPS [7]. LPS activates Toll-like receptor 4 (TLR4) of intestinal epithelial cells, triggering downstream signaling pathways, including transcription factor nuclear factor-κB (NF-κB) and mitogen-activated protein kinase (MAPK). This activation stimulates pro-inflammatory cytokines release, including tumor necrosis factor-α (TNF-α), interleukin-6 (IL-6), and interleukin-1β (IL-1β), promoting apoptosis

* Corresponding author.
E-mail addresses: davidliuyu@sina.com (Y. Liu); shtang@icmm.ac.cn (S. Tang); jxu0930@icmm.ac.cn (J. Xu)

https://doi.org/10.1016/S1875-5364(26)61206-X
Copyright © 2026, China Pharmaceutical University. Published by Elsevier B.V. All rights are reserved.

or necrosis of intestinal epithelial cells and further compromising the intestinal barrier [8]. The increased permeability allows more inflammatory cytokines and LPS to infiltrate the intestinal lamina propria, enter systemic circulation, and cross the BBB, resulting in exacerbating microglial activation. Moreover, microglial homeostasis relies on SCFAs produced by gut microbiota. Therefore, disrupting the microbiome balance can result in microglial activation, subsequently triggering neuroinflammation [9]. Our previous study observed that MCAO mice can induce intestinal dysfunction and release LPS, which subsequently exacerbates cerebral damage [10]. Many studies focused on elucidating mechanistic changes in the primary affected organ-brain using transcriptomic approaches in brain-gut axis research, while investigations into secondary affected organs-intestine, remain relatively scarce [11]. Thus, the exploration of mechanisms underlying intestinal injury following IS holds substantial clinical significance for improving IS prognosis and promoting neurological recovery.

Astragalus membranaceus (Fisch.) Bunge is a food and a traditional Chinese medicine with a long clinical history. Traditionally, *Astragalus membranaceus* has been valued for its effects in strengthening the spleen, increasing yang, and tonifying qi. It has also been widely used to treat IS and cardiovascular disease [12, 13]. A double-blind, randomized, controlled preliminary clinical study including 61 patients showed that *Astragalus membranaceus* improves the cognitive function of IS patients [14]. Astragalus polysaccharide (ASP) is a key bioactive compound from *Astragalus membranaceus*, exhibiting a wide range of pharmacological activities, including immunomodulatory, antioxidant, and anti-inflammatory [15]. Research has demonstrated that ASP may alleviate IS by modulating microglial function [16]. However, polysaccharides with higher molecular weights exhibit lower bioavailability, which makes it difficult for the host to directly absorb and utilize, and even more challenging to penetrate the brain [17]. Polysaccharides mainly function by influencing the gut microbiota, which can secrete various enzymes to interact with these polysaccharides, breaking them down into SCFAs, which are then absorbed by the human body [18]. For example, ASP supplementation can inhibit encephalomyelitis by regulating Th17/Treg through the microbiota-gut-brain axis [19]. ASP alleviates neuroinflammation by the MAPK/NF-κB signaling [20]. However, the regulatory mechanism of ASP on IS-induced intestinal dysfunction remains unclear.

This study determined that ASP modulates the microbiota-gut-brain axis to relieve IS-induced brain injury by integrating MCAO-induced animal models, antibiotics (ABX), and fecal microbiota transplantation (FMT) experiments. ASP's anti-ischemia effects are closely associated with its ability to modulate SCFA-producing bacteria, preserve intestinal barrier functions, and inhibit LPS leakage and microglial activation. These findings provide insights into ASP's anti-cerebral ischemia mechanism and lay a theoretical foundation for developing and applying ASP functional products from a neuroprotective perspective.

2. Materials and methods

2.1. Humans and animals

30 participants (17 normal participants and 13 IS patients) were recruited from the Dongzhimen Hospital of Beijing University of Chinese Medicine (Supplementary Table S1). The Ethics Committee of Dongzhimen Hospital of Beijing University of Chinese Medicine approved this study (Approval No. 2024DZMEC-379-02). Male C57BL/6J mice weighing 20–25g were purchased from Beijing Sipeifu Biotechnology Co., Ltd. (Beijing, China). The mice were housed in the specific pathogen-free (SPF) animal facilities at the Institute of Chinese Materia Medica, China Academy of Chinese Medical Sciences (Beijing, China). Guidelines for animal experiments were established by the Animal Research Committee of the China Academy of Chinese Medical Sciences (Approval No. 2024B375).

2.2. Chemicals and reagents

ASP (purity ≥ 90%, SA9790) was obtained from Beijing Solarbio Science & Technology Co., Ltd. [21]. ASP primarily consisted of glucose and xylose, et al [21]. According to previous studies, it was extracted from *Astragalus membranaceus* roots through water-ethanol precipitation followed by deproteinization [22]. Ginaton, as a positive control, was purchased from Dr. Willmar Schwabe GmbH & Co. KG.

Human LPS endotoxin (CSB-E09945h), mouse IL-6 (E-EL-M0044c), mouse LPS endotoxin (CSB-E13066m), and mouse IL-1β (E-EL-M0037c) ELISA kits were procured from Elabscience Biotechnology Co., Ltd. and Wuhan Huamei Biotech Co., Ltd., respectively. IBA-1 (ab5076), p-MAPK (4511), MAPK (8690), p-ERK (4370), ERK (4695), p-JNK (4668), JNK (9252), Claudin-1 (13050-1-AP), TLR4 (66350-1-lg), Occludin (27260-1-AP), NF-κB (80979-1-RR), ZO-1(AF5145), IL-6 (bs-4539R), MyD88 (bs-1047R), and IL-1β (26048-1-AP) were obtained from Abcam, Cell Signaling Technology, Proteintech, Affinity and Bioss. RIPA lysis buffer (R0010), PMSF protease inhibitor (P0100) and BCA assay kit (PC0020) were purchased from Solarbio Science & Technology Co., Ltd. Standards of SCFA, including acetic acid (CCFD200033), isohexanoic acid (CCEM500417), hexanoic acid (CCFD200155), isobutyric acid (CCEM500589), butanoic acid (CCFD200063), isovaleric acid (CCPD101342), valeric acid (CCFD200195), and propionic acid (CCFD200222), were all purchased from Cato Research Chemicals Inc.

2.3. Animal models and administration

The 90 mice were randomly divided into the sham (water), MCAO (water), ASP-L (low-dose ASP, 200 mg·kg^{-1}), ASP-M (medium-dose ASP group, 400 mg·kg^{-1}), ASP-H (high-dose ASP, 800 mg·kg^{-1}), and Ginaton (12.1 mg·kg^{-1}) groups (n = 15 per group). All mice were dosed orally once daily for 7 days. Then, as described in a previous study, the MCAO model was established [23, 24]. The mice were sacrificed, and then the brain, feces, colon, and serum were collected after 24 h of occlusion.

2.4. Antibiotics (ABX) and fecal microbiota transplantation (FMT) experiments

The 40 mice were randomly divided into the sham, MCAO, MCAO + ABX, and MCAO + ABX + ASP groups (n = 10 per group). The MCAO + ABX and MCAO + ABX + ASP groups received a broad-spectrum ABX consisting of ampicillin (200 mg·kg^{-1}), metronidazole (200 mg·kg^{-1}), vancomycin (100 mg·kg^{-1}), and neomycin sulfate (200 mg·kg^{-1}) for 7 days to deplete their gut microbiota [10]. Following the ABX treatment, the MCAO + ABX + ASP group received ASP *via* gavage for an additional 7 days, while the MCAO + ABX group was given an equivalent volume of water as a control. Subsequently, the MCAO model was established. After 24h of occlusion, the mice were sacrificed, and then the brain, feces, colon, and serum were collected.

For the FMT experiment, the 30 mice were randomly allocated into the MCAO + FMT and MCAO + FMT + ASP groups (n = 15 per group). All mice received daily oral administration of the ABX for 7 days. Fecal samples were then collected from 7 IS patients, with 1 g for each patient. All fecal samples were pooled together and prepared by diluting and mixing in sterile PBS to 100 mg·mL^{-1} fecal microbiota suspensions. 200 μL of suspension was intragastrically administered to recipient mice once daily for 7 days [25]. Following FMT treatment, the MCAO + FMT group

received water as a vehicle control, while the MCAO + FMT + ASP group was treated with ASP for an additional 7 days. Finally, the MCAO model was established in all experimental animals. After 24 h of occlusion, the mice were sacrificed, and then the brain, feces, colon, and serum were collected.

2.5. 2,3,5-Triphenyl tetrazolium chloride (TTC) staining, Nissl staining, and neurological deficient scores

After 24 h of occlusion, the Zea-Longa score method was performed for the neurological functional assessment [23,24]. Brain sections were sliced into 2 mm sections, incubated with 1% TTC, and fixed with 4% paraformaldehyde. Subsequently, the infarction rate was quantified as previously described [24]. Other brain tissues were fixed with 4% paraformaldehyde and embedded with paraffin. The paraffin sections were stained with 1% cresyl violet for Nissl staining.

2.6. Alcian blue/periodic acid-Schiff (AB-PAS) and hematoxylin and eosin (H&E) staining

The colon was fixed with 4% paraformaldehyde, followed by paraffin embedding and cutting sections. Then, the paraffin sections were dewaxed and stained with H&E constant dye kit (Servicebio, China) and AB-PAS dye set (Servicebio, China) for H&E and AB-PAS staining. Then, the pictures were captured and viewed *via* the NIKON DS-U3 imaging system and NIKON ECLIPSE E100 microscope.

2.7. Enzyme-linked immunosorbent assay (ELISA)

LPS, IL-6, and IL-1β in the colon, serum, and brain of mice or patients were quantified using ELISA kits. The procedure involved sequential incubation of samples with biotinylated-labeled secondary antibodies and HRP-conjugated reagents, followed by TMB substrate and stop solution. Absorbance was measured at 450 nm using a Spectra Max M5 microplate reader (Molecular Devices, USA).

2.8. Transcriptome sequencing and network pharmacology

Colon tissue in mice was prepared, and total RNA was extracted. The concentration and purity of total RNA were measured. cDNA libraries were constructed using Illumina® Stranded mRNA Prep, Ligation with total RNA. Genes with fold change ≥ 1.5 or ≤ 0.67 and P value < 0.05 were considered to be significantly differentially expressed genes (DEGs). InChI and SMILES information of ASP's constituents were taken from the PubChem database (http://pubchem.ncbi.nlm.nih.gov/) and uploaded to both the Swiss Target Prediction database (https://www.swisstargetprediction.ch/) and the BATMAN-TCM database (http://bionet.ncpsb.org/batman-tcm/) to predict the potential targets of ASP. All predicted targets and DEGs were analyzed for GO and KEGG pathway enrichment analyses using the Metascape platform (https://metascape.org/gp/index).

2.9. Metagenomic analysis

Total genomic DNA was isolated from fecal samples in mice, and the purity and concentration of DNA were assessed. The Covaris M220 system (Gene Company Limited, China) was employed to fragment the DNA to an average size of approximately 400 bp for the formation of paired-end libraries. The Illumina NovaSeq platform (Illumina Inc., San Diego, CA, USA) was utilized for paired-end sequencing. Gut microbial abundance data were normalized using the RPKM method. Data evaluation was conducted using the Majorbio Cloud Platform (www.majorbio.com). Functional annotation of gut microbiota was analyzed using the KEGG database (http://www.genome.jp/kegg/), and KEGG pathways were enriched at Level 3.

2.10. Targeted determination of SCFAs

Fecal samples of mice were added to 500 μL of extract (methanol∶water = 4∶1), ground, and low-temperature ultrasound. The supernatant was extracted and mixed with 3-nitrophenylhydrazine hydrochloride and 1-ethyl-3-(3-dimethylaminopropyl) carbodiimide hydrochloride (containing 6% Pyridine) solution. Then, a 50% acetonitrile solution was diluted and measured by LC-ESI-MS/MS (UHPLC-Qtrap).

2.11. Immunofluorescence staining (IF)

Brain sections were dewaxed, subjected to antigen retrieval, permeabilized, and blocked, followed by overnight incubation with primary antibodies at 4 °C（IBA-1, 1∶200). The corresponding secondary antibodies were applied and counterstained with DAPI for nuclear visualization. The VS120-S6-W digital slice scanner system (Olympus, Japan) was used to obtain the staining picture, and the IBA-1 positive rate was calculated.

2.12. Western blotting (WB)

Proteins were extracted from the brain and colon using RIPA lysis buffer supplemented with phosphatase and protease inhibitors and quantified *via* a BCA assay. After separation by SDS–PAGE, proteins were transferred to PVDF membranes, blocked with 5% skim milk, and incubated overnight with primary antibodies: p-MAPK and MAPK (1∶1000), p-JNK and JNK (1∶1000), p-ERK and ERK (1∶1000), ZO-1 (1∶1000), MyD88 (1∶1000), Occludin (1∶1000), NF-κB (1∶10000), IL-1β (1∶500), Claudin-1 (1∶1000), TLR4 (1∶5000), and IL-6 (1∶1000). Following secondary antibody incubation, protein bands were visualized using ECL and imaging with a Tanon 4600 gel imaging system (Tanon Science & Technology, China).

2.13. Statistical analysis

GraphPad Prism 8.0.2 was employed for statistical analysis. One-way ANOVA was used to compare multiple groups, while Student's t-test was applied to compare two groups. Data are presented as mean ± SD. $P < 0.05$ was regarded as significant.

3. Results

3.1. ASP ameliorated infarction rate, neurological deficient scores, and neuron loss in MCAO mice with dose dependence

To explore the protective effects of ASP against MCAO, infarction rate, neurological deficient scores, and neuronal damage were determined (Fig. 1A). Compared with the infarction rate of 72.15% ± 7.13% in the MCAO group, the infarction rate in the ASP-M, ASP-H, and Ginaton groups was 49.28% ± 8.84%, 41.26% ± 5.47%, and 49.72% ± 11.78%, respectively ($P < 0.01$, Figs. 1B–1C). Compared with the sham group, neurological deficient scores were higher after MCAO. In contrast, compared with the MCAO group, these scores were lower in the ASP-M, ASP-H, and Ginaton groups ($P < 0.05$, Fig. 1D). Although there were no statistically significant differences in infarction rate or neurological deficient scores in the ASP-L group, both measures showed a decreasing trend. Compared with the sham group, Nissl staining revealed the loss of neurons in the cortex and hippocampus after MCAO. Compared with the MCAO group, the neuron loss was

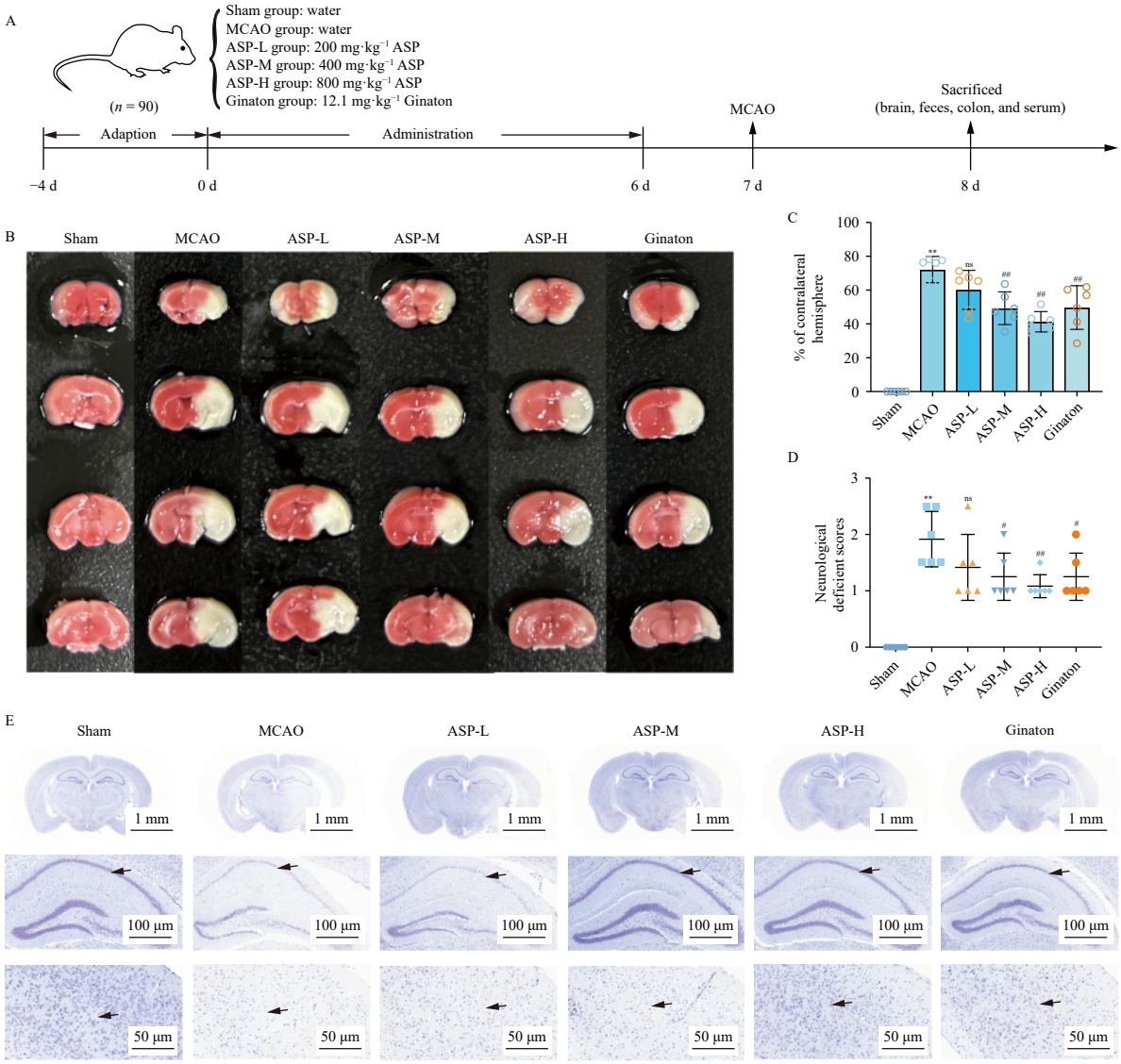


Fig. 1 ASP ameliorated infarction rate, neurological deficient scores, and neuron loss in MCAO mice. (A) Experimental design flow chart. (B) TTC staining images. (C) Infarction rate (n = 6). (D) neurological deficient scores (n = 6). (E) Nissl staining images, scale bar: 1 mm, 100 μm, 50 μm. Results are expressed as mean ± SD. $^{\#}P < 0.05$, $^{\#\#}P < 0.01$ *vs* MCAO group, ns indicates no significant difference; $^{**}P < 0.01$ *vs* sham group. Data were analyzed using one-way ANOVA with Bonferroni's post-hoc test.

ameliorated after different doses of ASP and Ginaton treatment (Fig. 1E). These results suggested that ASP can ameliorate neurological deficient scores, infarction rate, and neuron loss, and ASP-H was used in further studies.

3.2. ASP alleviated neuroinflammation and BBB injury in MCAO mice

When BBB is disrupted after IS, inflammatory cytokines enter the brain, inducing neuroinflammation. In turn, neuroinflammation impairs BBB function, enhancing its permeability [26]. WB analysis revealed that compared with the sham group, tight junction protein expression (Occludin and Claudin-1) and inflammatory cytokine levels (IL-1β and IL-6) in the brain were significantly downregulated and upregulated after MCAO, respectively, and ASP reversed these alterations ($P < 0.05$, Figs. 2A–2F). ELISA results indicated that MCAO mice had higher levels of serum IL-1β compared with the sham group, levels that were attenuated by treatment with ASP and Gination ($P < 0.05$, Fig. 2G). IBA-1 is a marker for microglial activation, which is closely related to neuroinflammation [27]. IBA-1 positive rate was increased after MCAO, while ASP reduced its levels ($P < 0.05$, Figs. 2H–2I). Therefore, ASP can alleviate neuroinflammation and BBB injury.

3.3. ASP restored intestinal barrier integrity in MCAO mice

H&E and AB-PAS staining revealed intact colonic mucosa with well-organized crypts in the sham group, whereas MCAO mice exhibited disrupted epithelial and crypt architecture. Compared with the MCAO group, ASP and Ginaton treatment significantly ameliorated these structural damages (Figs. 3A-3B). According to WB, the MCAO group's colonic ZO-1, Occludin, and Claudin-1 were lower than those of the sham group. These protein expressions were upregulated following ASP treatment ($P < 0.05$, Figs. 3C–3F). MCAO mice upregulated colonic IL-1β levels compared with the sham group, and ASP suppressed IL-1β levels compared with the MCAO group ($P < 0.05$, Figs. 3G–3H). MCAO mice had higher levels of colonic IL-1β and IL-6 by ELISA. In contrast, ASP and Gination reduced these inflammatory cytokine levels ($P < 0.05$, Figs. 3I–3J). Therefore, ASP can restore intestinal barrier integrity.

3.4. ASP changed gut microbiota composition in MCAO mice

To explore the regulation of ASP in the gut microbiota, the composition of gut microbiota was studied *via* Metagenomic analysis between the sham, MCAO, and ASP-H groups. As shown in

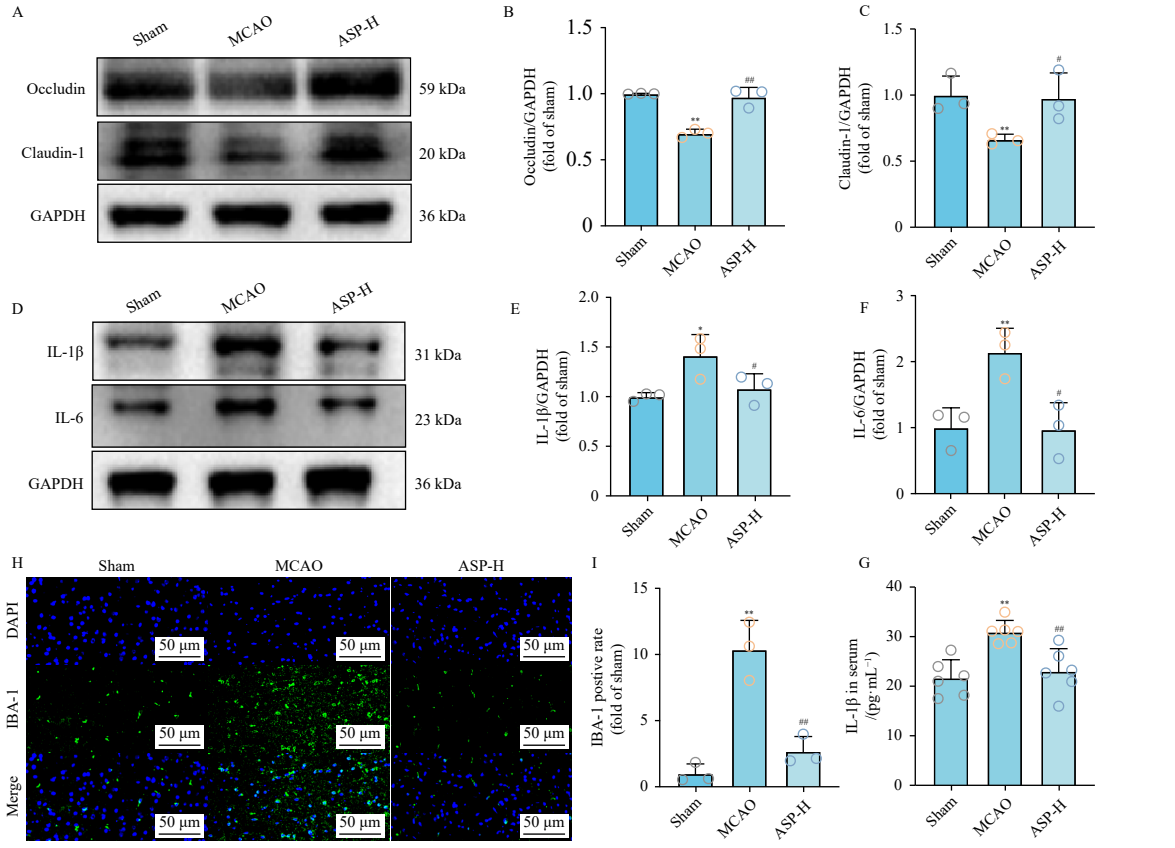


Fig. 2 ASP alleviated neuroinflammation and BBB injury in MCAO mice. (A) Occludin and Claudin-1 images in the brain by WB. Brain (B) Occludin and (C) Claudin-1 expressions (n = 3). (D) Brain IL-1β and IL-6 images by WB. Brain (E) IL-1β and (F) IL-6 levels (n = 3). (G) Serum IL-1β levels (n = 6). (H) IBA-1 images by IF, scale bar: 50 μm. (I) IBA-1 positive rate (n = 3). Results are expressed as mean ± SD. $^{\#}P < 0.05$, $^{\#\#}P < 0.01$ *vs* MCAO group; $^{*}P < 0.05$ and $^{**}P < 0.01$ *vs* sham group. Data were analyzed using one-way ANOVA with Bonferroni's post-hoc test.

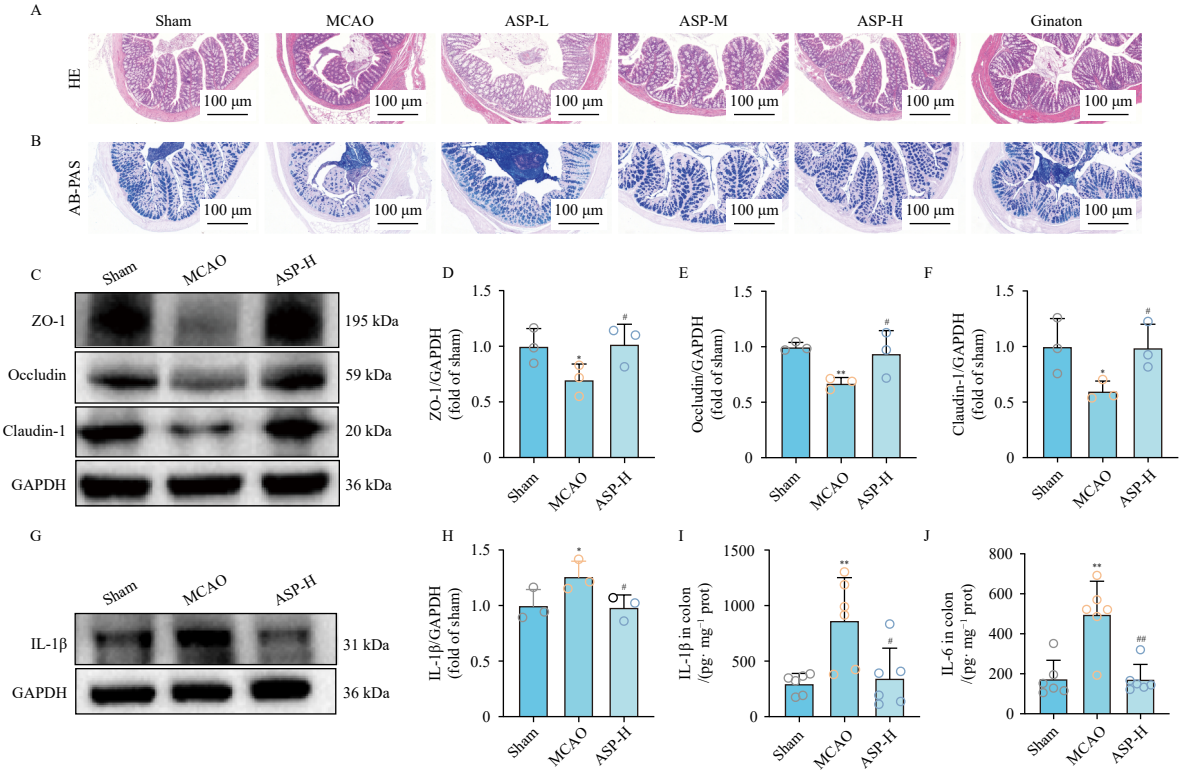


Fig. 3 ASP restored intestinal barrier integrity in MCAO mice. (A–B) Colonic H&E and AB-PAS staining, scale bar: 100 μm. (C) ZO-1, Claudin-1, and Occludin images by WB. Colonic (D) ZO-1, (E) Occludin, and (F) Claudin-1 expressions (n = 3). (G) Colonic IL-1β images by WB. (H) Colonic IL-1β levels (n = 3). Levels of colonic (I) IL-1β and (J) IL-6 by ELISA (n = 6). Results are expressed as mean ± SD. $^{\#}P < 0.05$, $^{\#\#}P < 0.01$ *vs* MCAO group; $^{*}P < 0.05$ and $^{**}P < 0.01$ *vs* sham group. Data were analyzed using one-way ANOVA with Bonferroni's post-hoc test.

Figs. 4A–4C, alpha diversity revealed that community diversity and richness were reduced by MCAO, while ASP reversed these indices. Beta diversity revealed distinct clustering patterns among groups, with ASP-treated mice showing more similarity to the sham group than to MCAO mice (Fig. 4D). The predominant phyla included Firmicutes, Bacteroidota, Verrucomicrobia, and Proteobacteria (Fig. 4E). At the family level, Muribaculaceae, Bacteroidaceae, Enterobacteriaceae, and Lachnospiraceae dominated the microbial composition (Fig. 4F). A significant reduction in the Firmicutes/Bacteroidota (F/B) ratio in MCAO mice was observed, which was subsequently elevated after ASP (Fig. 4G). At the genus level, beneficial bacteria of the intestinal barrier and BBB (*Anaerostipes, Lachnoclostridium*), anti-inflammatory bacteria (*Lachnoclostridium, Anaerostipes, Anaerobutyricum, Caproiciproducens*), SCFA-produced bacteria (*Lachnoclostridium*, *Mediterraneibacter*, *Sporofaciens*, *Anaerostipes*, *Anaerobutyricum*, and *Caproiciproducens, Eisenbergiella*) were significantly downregulated [28-34], whereas pro-inflammatory bacteria (*Burkholderia*) were notably upregulated following MCAO [35]. Gut microbiota's dysbiosis was effectively restored following ASP treatment (Fig. 4H).

Spearman correlation analysis demonstrated negative associations between beneficial bacteria (*Anaerostipes, Anaerobutyricum*, *Lachnoclostridium, Caproiciproducens*, *Mediterraneibacter*, *Sporofaciens*, and *Eisenbergiella*) and pro-inflammatory cytokines (LPS, IBA-1, IL-6, and IL-1β), suggesting that ASP-mediated modulation of gut microbiota may contribute to its anti-neuroinflammatory effects (Fig. 4I). Gut microbiota's functions were predicted using the KEGG pathway analysis, which revealed significant upregulation of lipopolysaccharide biosynthesis and the MAPK signaling pathway in MCAO mice, both of which were normalized following ASP (Figs. 4J–4K). These results suggest that ASP-mediated differential bacteria may regulate lipopolysaccharide biosynthesis and the MAPK signaling pathway.

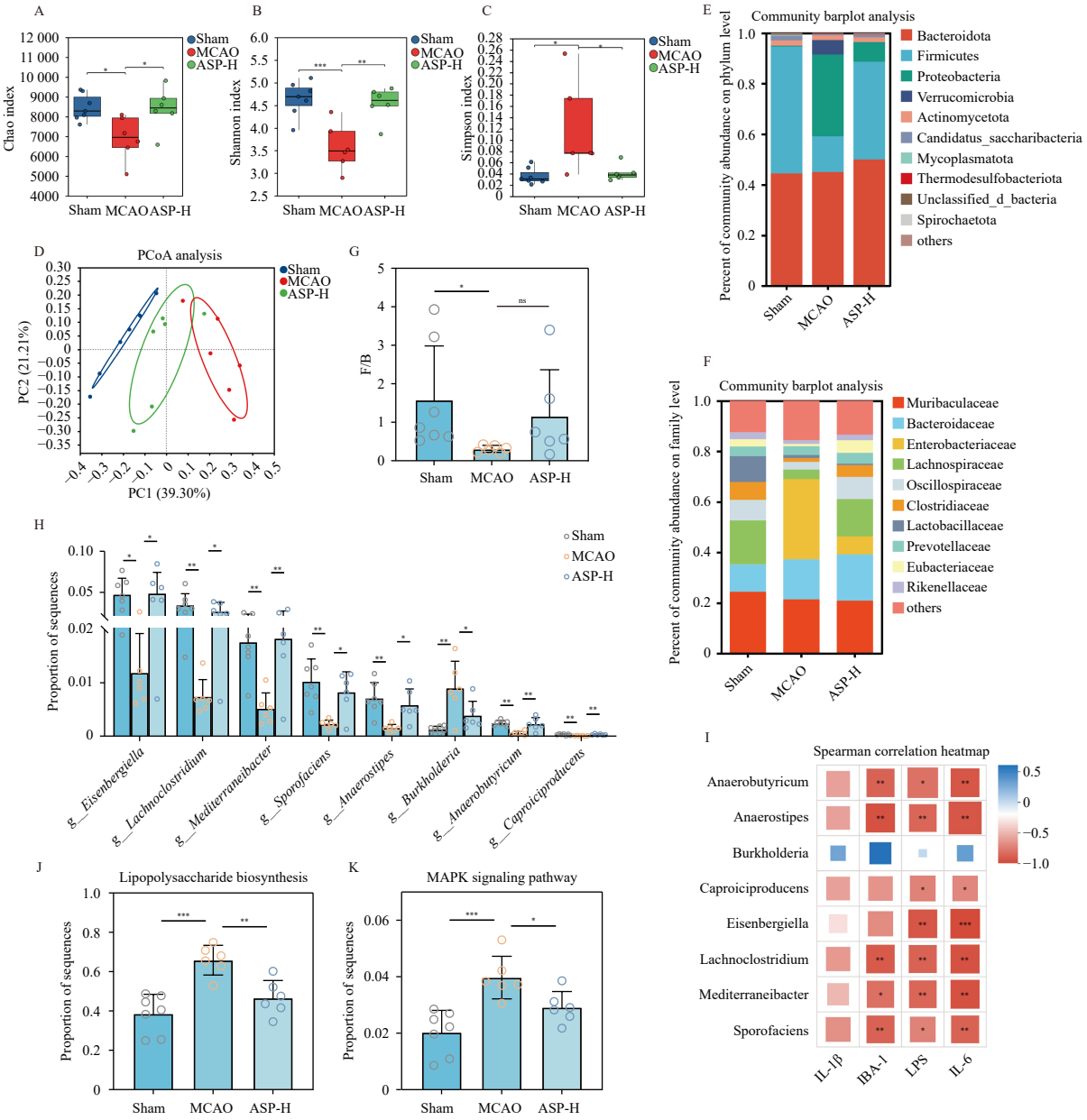


Fig. 4 ASP changed gut microbiota composition in MCAO mice. Alpha diversity analysis by (A) Chao, (B) Shannon, and (C) Simpson indices. (D) PCoA analysis. Relative abundance at the (E) phylum and (F) family levels. (G) F/B ratio. (H) Relative abundance of different bacterial genera. (I) Spearman correlation heatmap between neuroinflammation and different bacterial genera. Differential pathways of (J) lipopolysaccharide biosynthesis and (K) MAPK signaling pathway. Results are expressed as mean ± SD (n = 6–7). $^{*}P < 0.05$, $^{**}P < 0.01$, and $^{***}P < 0.001$ *vs* MACO group; ns indicates no significant difference. Data were analyzed using one-way ANOVA with Bonferroni's post-hoc test.

3.5. ASP increased SCFA concentration in the feces of MCAO mice

For the investigation of the role of ASP in SCFAs, the concentrations of SCFAs in fecal samples of mice were determined *via* LC-ESI-MS/MS. Compared with the sham group, MCAO induced a significant reduction in total SCFA content, which was effectively reversed by ASP (Fig. 5A). MCAO notably decreased propanoic acid, acetic acid, valeric acid, and butanoic acid concentrations while increasing isohexanoic acid. Compared with the MCAO group, ASP significantly elevated acetic acid, valeric acid, hexanoic acid, and butanoic acid concentrations (Figs. 5B–5I).

To further evaluate the relationships among SCFAs, differential bacteria, intestinal barrier function, BBB integrity, and neuroinflammation, Spearman correlation analysis was performed. SCFAs were positively correlated with anti-inflammatory bacteria, intestinal barrier, and BBB integrity, whereas they were negatively correlated with pro-inflammatory bacteria and neuroinflammation (Fig. 5J). These findings suggest that microbiota-derived SCFAs may affect the intestinal barrier function, BBB integrity, and neuroinflammation.

3.6. ASP suppressed the LPS-TLR4-MAPK pathway in the colon of MCAO mice

After ischemic stroke, the occurrence of inflammation, disruption of the intestinal barrier, LPS translocation, and reduction of SCFAs are important factors leading to the aggravation of brain injury [36]. Transcriptomic analysis revealed 2595 differentially expressed genes (DEGs) between the MCAO and sham groups, comprising 1,091 upregulated and 1,504 downregulated genes (Supplementary Fig. S1). ASP's potential targets were predicted using the Swiss Target Prediction and BATMAN-TCM databases. DEGs are mainly related to inflammation, intestinal barrier, response to LPS, and response to SCFAs (Fig. 6A). GO analysis revealed that biological processes (BP) related to the fatty acid metabolic process, inflammatory response, neuron projection development, and response to bacterium were enriched among these targets (Fig. 6B). KEGG enrichment analysis identified primary pathways associated with Wnt, JAK-STAT, MAPK, and PPAR signaling pathways, fatty acid degradation, and fatty acid biosynthesis (Fig. 6C). Among them, the MAPK signaling pathway had the smallest *P* value compared with other signaling pathways, indicating the MAPK signaling pathway plays an important role in regulating intestinal injury after IS.

The MAPK pathway serves a pivotal relationship in modulating intestinal permeability and inflammation. Specifically, LPS triggers the activation of the MAPK pathway through TLR4-mediated signaling, leading to increased intestinal permeability and inflammatory processes [37]. ELISA results indicated that MCAO mice had higher serum, brain, and colonic LPS levels than the sham group. In contrast, ASP reduced LPS levels in serum, brain, and colonic (Figs. 6D–6F). WB results demonstrated that compared with the sham group, colonic TLR4, MyD88, NF-κB, p-MAPK/MAPK, p-JNK/JNK, and p-ERK/ERK expressions were increased after MCAO, and these proteins were decreased after ASP (Figs. 6G–6N). These results indicate that ASP can alleviate MCAO-induced colonic injury by suppressing the LPS-TLR4-MAPK pathway.

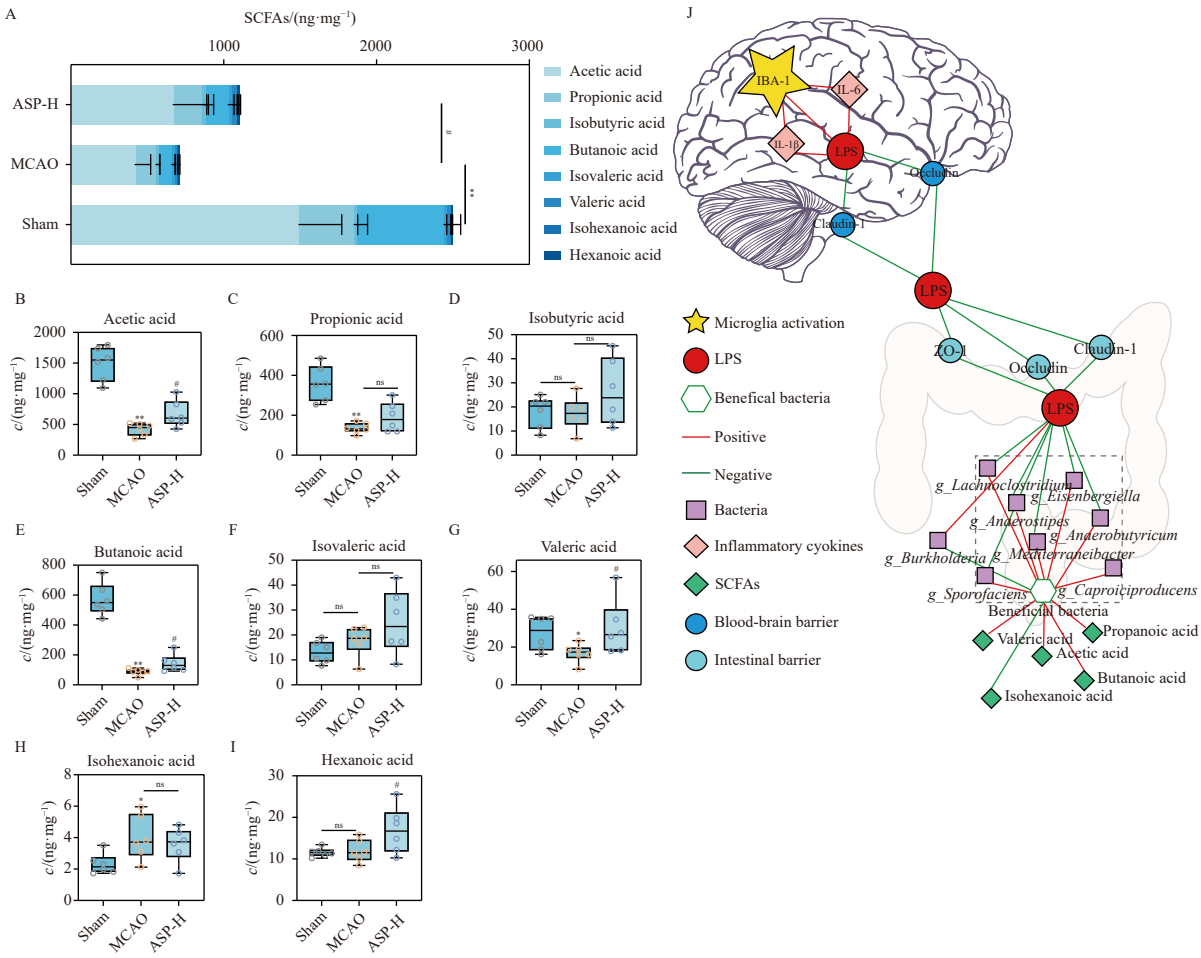


Fig. 5 ASP increased SCFA concentration in MCAO mice. The concentration of (A) total SCFAs, (B) acetic acid, (C) propanoic acid, (D) isobutyric acid, (E) butanoic acid, (F) isovaleric acid, (G) valeric aid, (H) isohexanoic acid, and (I) hexanoic acid. (J) Spearman correlation heatmap between SCFAs, bacterial genera, intestinal barrier function, BBB integrity, and neuroinflammation. Results are expressed as mean ± SD (n = 6). ns indicates no significant difference; $^{\#}P < 0.05$ *vs* MCAO group; $^{*}P < 0.05$ and $^{**}P < 0.01$ *vs* sham group. Data were analyzed using one-way ANOVA with Bonferroni's post-hoc test.

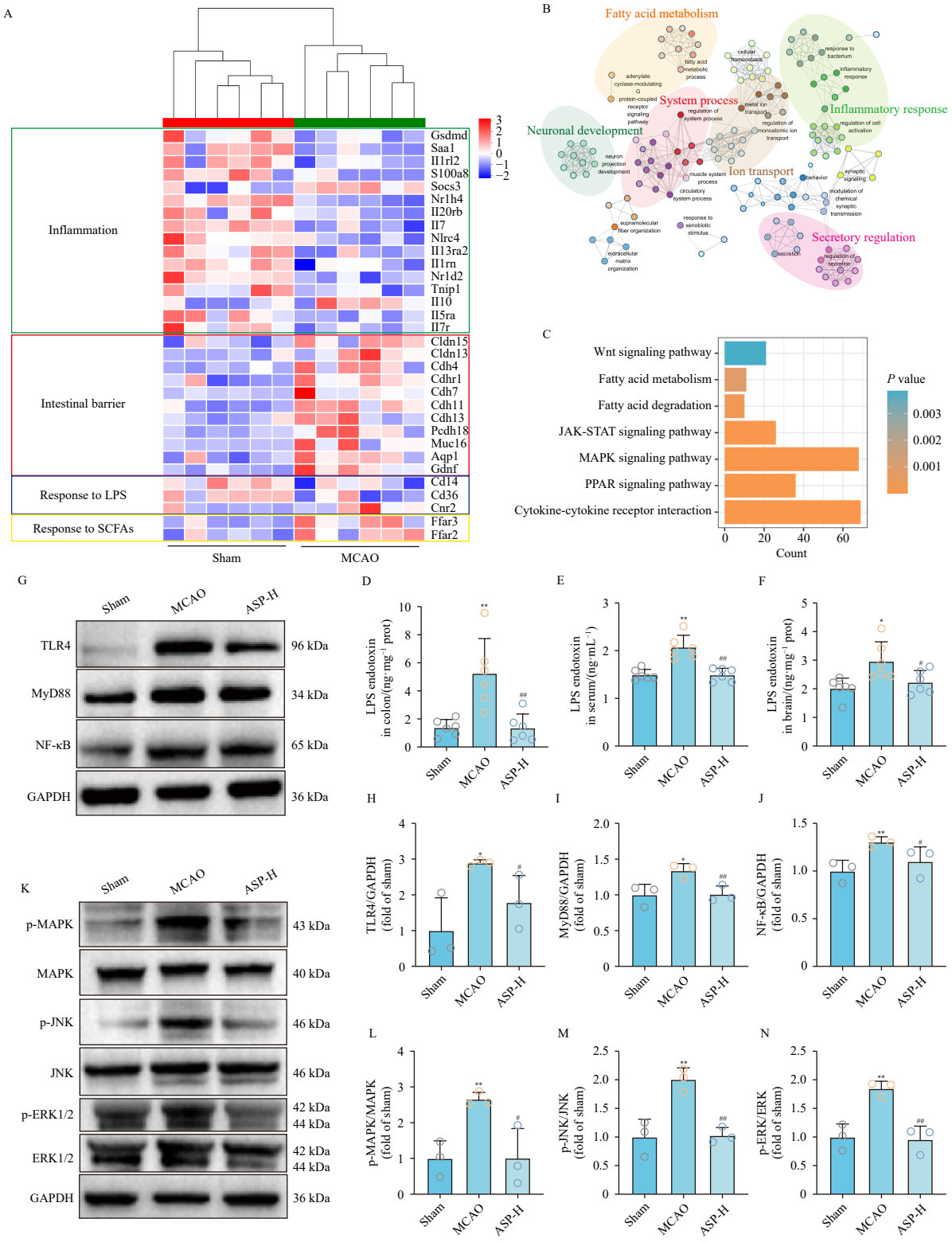


Fig. 6 ASP suppressed the LPS-TLR4-MAPK pathway in the colon of MCAO mice. (A) Heatmap of DEGs enriched in inflammation, intestinal barrier, response to LPS, and response to SCFAs (n = 6). (B) BP network. (C) KEGG pathways. Mouse LPS levels in the (D) colon, (E) serum, and (F) brain (n = 6). (G) Colonic TLR4, MyD88, and NF-κB images by WB. The expression of colonic (H) TLR4, (I) MyD88, (J) NF-κB (n = 3). (K) Colonic p-MAPK/MAPK, p-JNK/JNK, and p-ERK/ERK images by WB. The expression of colonic (L) p-MAPK/MAPK, (M) p-JNK/JNK, and (N) p-ERK/ERK (n = 3). $^{\#}P < 0.05$, $^{\#\#}P < 0.01$ *vs* MCAO group; $^{*}P < 0.05$ and $^{**}P < 0.01$ *vs* sham group. Data were analyzed using one-way ANOVA with Bonferroni's post-hoc test. Results are expressed as mean ± SD.

3.7. ASP lost the ability to alleviate cerebral injury in MCAO mice after the elimination of gut microbiota

To investigate whether gut microbiota influences ASP's therapeutic effects on IS by administering ABX to delete gut microbiota (Fig. 7A). As shown in Figs. 7B–7D, alpha diversity revealed that community diversity and richness were significantly down-regulated after ABX treatment. PCoA analysis showed that there was a distinct cluster in each group (Fig. 7E). Most of the gut microbiota was effectively eliminated at the phylum level after ABX treatment (Fig. 7F). Importantly, no significant differences were observed in body weight (Fig. 7G), neurological defi-

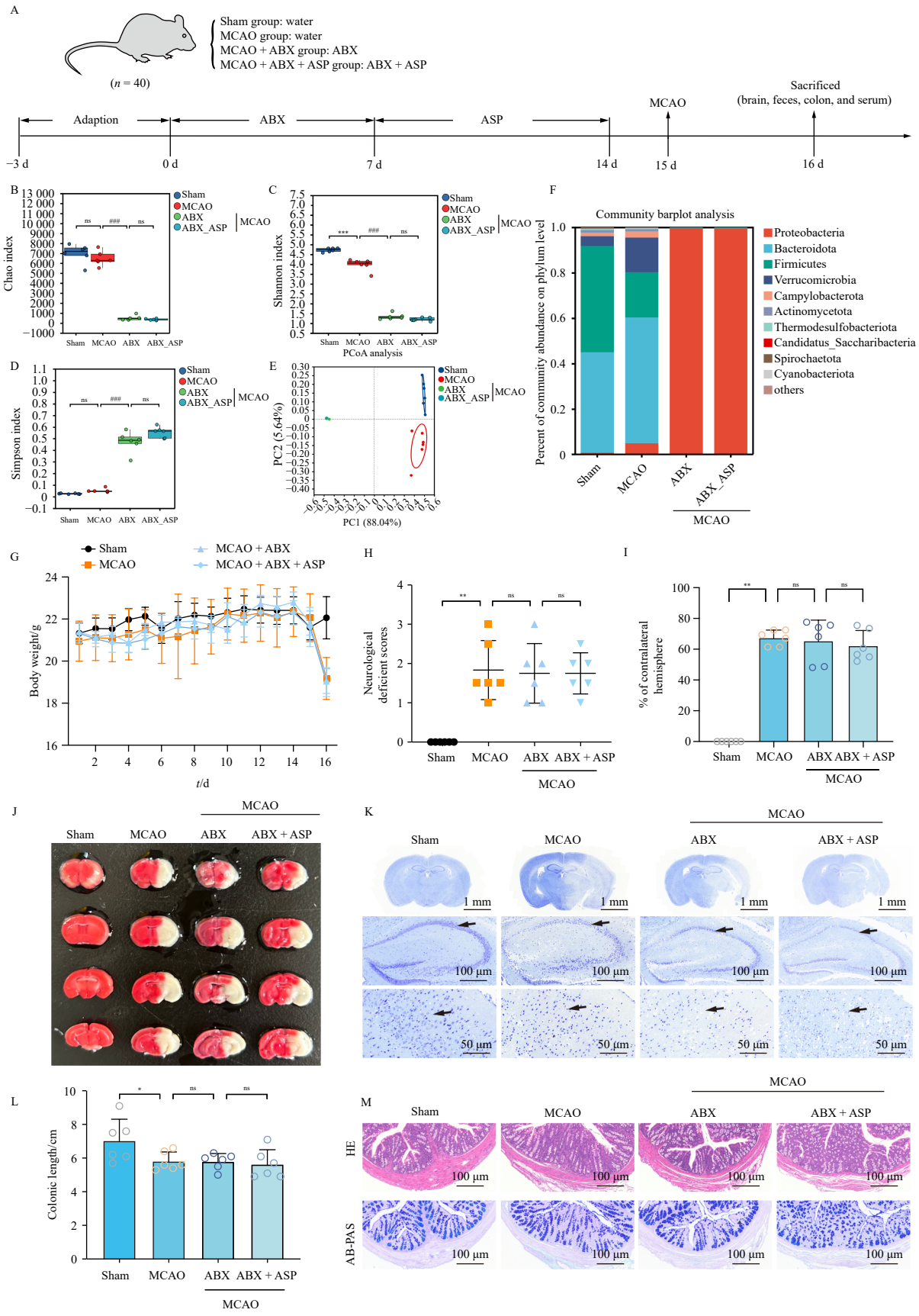


Fig. 7 ASP lost the ability to alleviate brain injury in MCAO mice after the elimination of gut microbiota. (A) Experimental design flow chart. (B) Chao, (C) Shannon, and (D) Simpson indices (n = 6). (E) PCoA analysis (n = 6). (F) Relative abundance at the phylum levels (n = 6). (G) Body weight (n = 8). (H) Neurological deficient scores (n = 6). (I) Infarction rate (n = 6). (J) TTC staining images. (K) Nissl staining images, scale bar: 1 mm, 100 μm, 50 μm. (L) Colonic length (n = 6). (M) Colonic AB-PAS and H&E staining, scale bar: 100 μm. Results are expressed as mean ± SD. ns indicates no significant difference; $^{###}P < 0.001$ *vs* MCAO group; $^{*}P < 0.05$ and $^{***}P < 0.001$ *vs* sham group. Data were analyzed using one-way ANOVA with Bonferroni's post-hoc test.

cient scores (Fig. 7H), infarction rate (Figs. 7I–7J), neuronal damage (Fig. 7K), colonic length (Fig. 7L), and colonic structures (Fig. 7M) of MCAO + ABX and MCAO + ABX + ASP groups following gut microbiota elimination. These results suggest that ASP-dependent gut microbiota alleviated brain injury in MCAO mice.

3.8. ASP alleviated cerebral injury in MCAO mice transplanted with microbiota from IS patients

To further investigate ASP-modulated gut microbiota's impact on IS, FMT was conducted using fecal samples from IS patients, followed by ASP administration (Fig. 8A). ELISA results indicated that serum LPS in human patients with IS was significantly elevated compared with normal participants (Fig. 8B). The MCAO + FMT + ASP group demonstrated notable improvements compared to the MCAO + FMT group, including increased body weight (Fig. 8C), reduced neurological deficient scores (Fig. 8D), lower infarction rate (Figs. 8E–8F), and attenuated neuronal damage (Fig. 8G). Meanwhile, the colonic length was longer (Fig. 8H), and colonic structures (Fig. 8I) were significantly restored. Inflammatory cytokines (IL-1β and IL-6) and LPS levels in the colon, brain, and serum were suppressed (Figs. 8J–8L). Metagenomic analysis showed that Firmicutes, Bacteroidota, Proteobacteria at the phylum levels, and Muribaculaceae, Bacteroidaceae, Prevotellaceae at the family levels dominated the microbial composition (Figs. 8M–8N). Compared to the MCAO + FMT group, the F/B ratio and beneficial bacteria of anti-inflammatory and SCFA-producing (*g_Anaerobutyricum* and *g_Caproiciproducens*) were significantly upregulated in the MCAO + FMT + ASP group (Figs. 8O–8Q). And elevated levels of tight junction proteins (Occludin, Claudin-1) of the MCAO + FMT + ASP group were observed in the brain and colon (Figs. 8R–8S). Additionally, the MCAO + FMT + ASP group had lower expression of colonic TLR4, MyD88, NF-κB, p-MAPK/MAPK, p-JNK/JNK, and p-ERK/ERK (Fig. 8T), as well as a decreased IBA-1 positive rate (Figs. 8U–8V). These results demonstrate that ASP can alleviate cerebral and colonic injury in MCAO mice transplanted with microbiota from IS patients.

4. Discussion

IS, characterized by cerebral hypoperfusion, leading to neurological dysfunction and parenchymal necrosis, poses a significant clinical challenge with substantial socioeconomic burdens due to its high incidence and debilitating consequences. Emerging research has elucidated the crucial role of the microbiota-gut-brain axis in stroke pathophysiology, particularly highlighting gut microbiome's effect in disease progression [38]. Among various therapeutic candidates, ASP has garnered interest as its dual pharmacological qualities, including neuroprotection and anti-inflammatory effects, positioning it as a potential intervention for neurological disorders [39]. This study employed MCAO-induced animal models, ABX treatment, and FMT experiments to investigate the neuroprotective mechanisms of ASP against IS. The results demonstrated that ASP treatment exerted neuroprotective effects, evidenced by a reduction of infarction rate, improvement in neurological deficient scores, preservation of Nissl body density, suppression of microglial activation, modulation of systemic inflammatory cytokines, restoration of intestinal barrier, and BBB function *via* the microbiota-gut-brain axis.

Recent studies indicate that IS not only directly causes CNS damage but also intestinal dysfunction mediated by the microbiota-gut-brain axis. Importantly, intestinal functional recovery directly affects neuroinflammation and neurological repair processes. Therefore, improving intestinal dysfunction is crucial for the prognosis of IS. Tight junction proteins, as components of the intestinal barrier, maintain the structural stability of intestinal epithelial cells by mediating cell-cell adhesion, which can prevent direct interaction between detrimental microbial byproducts like LPS and the epithelial cells, thereby reinforcing the intestinal barrier [40]. Notably, microbial imbalance has emerged as a critical factor contributing to intestinal dysfunction, while targeted microbial modulation demonstrates therapeutic potential in mitigating CNS disease-induced gut barrier impairment. Several studies indicated that microbial community structures were abnormal in MCAO mice, and MCAO exacerbates intestinal dysfunction by damaging bacterial abundance [41, 42]. Moreover, the abundance of Firmicutes is reduced in patients with IS and MCAO mice, and Firmicute abundance is inversely associated with intestinal barrier injury [43]. *Caproiciproducens* and *Anaerobutyricum* belong to the phylum Firmicutes, which can produce SCFA [28]. *Anaerobutyricum*, as a beneficial bacterium, exerts an important role in intestinal and CNS inflammation [33]. *Caproiciproducens* is a main producer of butyrate and caproate. Butyrate can regulate intestinal barrier function and is a metabolic substrate for colonic epithelial cells [34]. A clinical study revealed that patients with IS exhibit significant depletion of butyrate-producing bacterial taxa in gut microbiota and a marked reduction in acetic acid concentration [25, 44]. Additionally, gut microbiota homeostasis's disruption can lead to elevated LPS production within intestinal epithelial cells, subsequently causing intestinal barrier dysfunction. The recognition of LPS and other non-microbial ligands by TLR4 involves multiple cell surface proteins, activates inflammatory signaling pathways, including NF-κB and MAPK cascades [45]. Studies have shown that intestinal barrier dysfunction can be alleviated by suppressing the TLR4/MAPK signaling [46]. Upon access to the circulatory system and migration to cerebral tissues, LPS induces a series of pathological changes, including BBB disruption, inflammatory cell infiltration, and microglial activation [47]. Serum LPS levels in IS patients are higher than those of healthy individuals and correlate with worse outcomes in patients with IS in a clinical study [48]. Our findings demonstrate that MCAO-induced cerebral ischemia triggers intestinal dysfunction, characterized by gut microbiota dysbiosis, decreased SCFAs, elevated colonic LPS and proinflammatory cytokines, and impaired intestinal barrier integrity. Further transcriptomics revealed that the mechanism of MCAO-induced intestinal dysfunction is to activate the colonic TLR4/MAPK pathway. Furthermore, MCAO-induced intestinal dysfunction exacerbates neuroinflammation, as evidenced by BBB disruption, increased LPS and inflammatory cytokines in the brain, and microglial activation.

In recent decades, polysaccharides have garnered significant attention for their potent pharmacological activities and minimal side effects in preventing and treating complex diseases, including neurological and metabolic diseases. However, polysaccharides are difficult to be directly digestible and absorbable by the human body, resulting in low bioavailability [49]. Studies showed that polysaccharides mainly exert pharmacological effects *via* the gut microbiota. Specifically, after entering the human body, polysaccharides are absorbed by the colon, promoting and enhancing the richness and diversity of gut microbiota. Meanwhile, gut microbiota ferments and utilizes polysaccharides, promoting the production of beneficial metabolites (SCFAs), which exert antioxidant and anti-inflammatory effects [18]. The structure-activity relationship of polysaccharides encompasses the influence of primary and advanced structures and physicochemical properties on the biological activity of polysaccharides [50]. ASP, classified into dextran and heteropolysaccharides, mainly consists of glucose, galactose, arabinose, and rhamnose connected by α- or β-glycosidic bonds. For example, purified ASP obtained *via* water extraction and column purification is primarily glucan with small amounts of galactose and arabinose [51]. ASP's biological activity is associated with molecular weight, sugar chain branching degree, and sugar group composition. ASP's water solubility or biological activity can be enhanced by chemical modifications such as sulfa-

tion, carboxymethylation, or acetylation [52]. The honey-processing procedure led to the degradation of ASP, as evidenced by a significant reduction in their molecular weights. Notably, the resulting degraded fractions exhibited enhanced anti-inflammatory activity compared to the original ASP [53]. A study isolated two novel polysaccharides (APS-B1 and APS-A1). Structural analysis revealed that APS-A1 possesses a backbone of 1,4-α-D-Glcp with a branch of 1,4,6-α-D-Glcp every ten residues. APS-B1 consists of

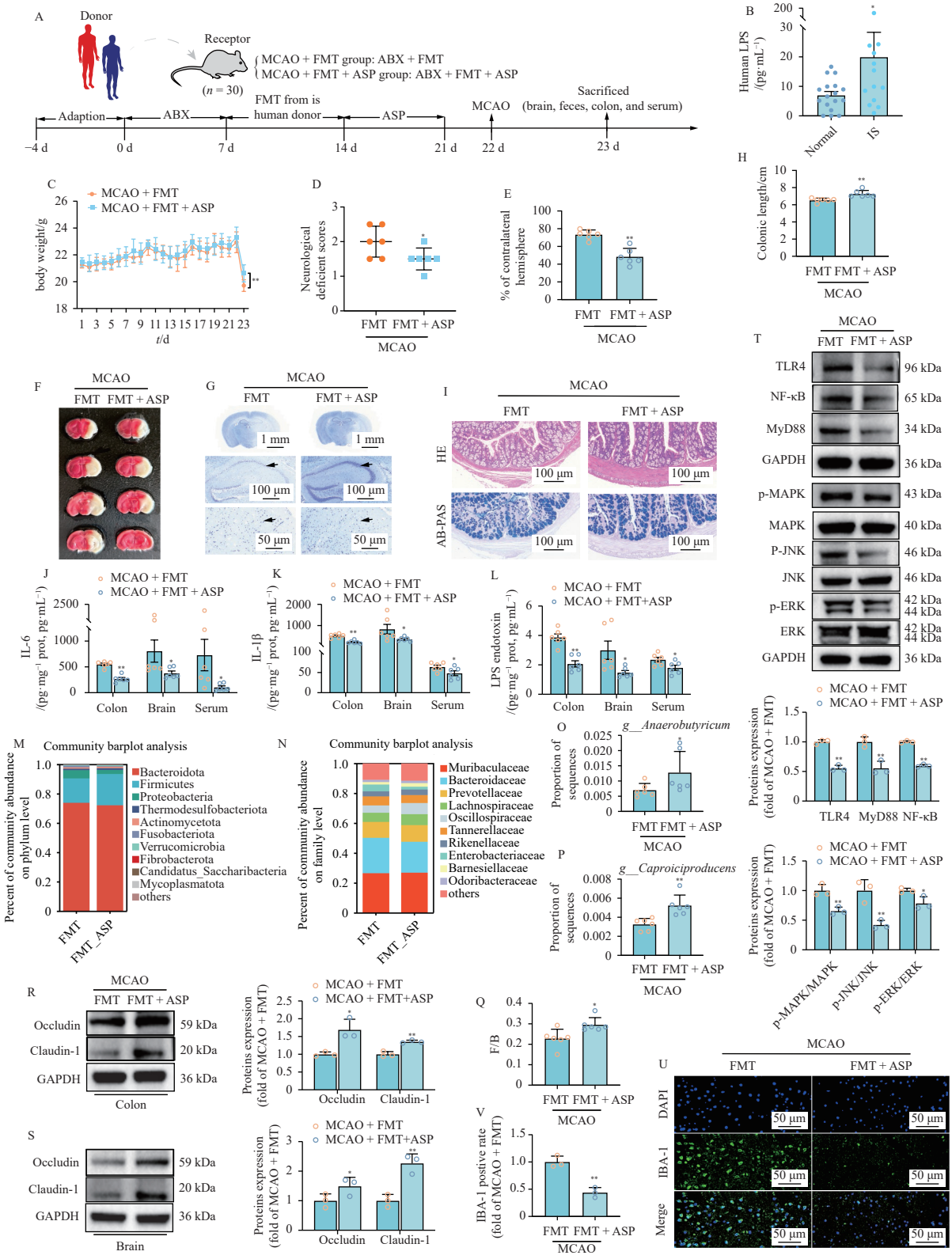


Fig. 8 ASP reinstated cerebral injury in MCAO mice transplanted with microbiota from IS patients. (A) Experimental design flow chart. (B) Human LPS levels in the serum (n = 13–17). (C) Body weight (n = 8). (D) Neurological deficient scores (n= 6). (E) Infarction rate (n = 6). (F) TTC staining images. (G) Nissl staining images, scale bar: 1 mm, 100 μm, and 50 μm. (H) Colonic length (n= 6). (I) Colonic H&E and AB-PAS staining, scale bar: 100 μm. (J) IL-6, (K) IL-1β and (L) LPS levels by ELISA (n = 6). Relative abundance at the (M) phylum and (N) family levels (n = 6). Relative abundance of (O) *g_Anaerobutyricum* and (P) *g_Caproiciproducens* (n = 6). (Q) F/B ratio (n = 6). Representative images and quantification of ZO-1, Claudin-1, and Occludin in the (R) colon and (S) brain (n = 3). (T) Representative images and quantification of colonic TLR4, MyD88, and NF-κB. p-MAPK/MAPK, p-JNK/JNK, and p-ERK/ERK (n = 3). (U) Brain IBA-1 images by IF, scale bar: 50 μm. (V) IBA-1 positive rate (n = 3). Data are presented as mean ± SD. $^{*}P < 0.05$ and $^{**}P < 0.01$ *vs* MCAO + FMT group. Student's *t*-test.

glucose, arabinose, and galactose. Its backbone is primarily built from 1,4-α-D-Glcp, 1,4,6-α-D-Glcp, and 1,5-α-L-Araf, while the side chains are formed by 1,6-α-D-Galp and T-α/β-Glcp. Bioactivity evaluation demonstrated that both APS-A1 and APS-B1 exhibit significant anti-inflammatory potential [54]. The presence of β-D-(1→3)-galactan bearing β-D-(1→6)-galacto-oligosaccharide side chains can mediate intestinal immunomodulation [55]. Studies have demonstrated that ASP has significant potential in neuroprotection, which can reduce IS-induced brain damage by regulating microglial function [16]. By eliminating free radicals and inhibiting inflammatory cytokines, ASP can alleviate neuroinflammation and help maintain BBB integrity, preventing harmful substances from entering the brain and reducing brain edema and nerve cell damage [19]. Additionally, ASP can regulate the microbiota-brain-gut axis to alleviate LPS-induced neuroinflammation by regulating gut microbiota composition [20]. Therefore. Most previous studies have focused on the mechanism of the primary organ - the brain, while neglecting the secondary organ - the intestine. Our study focused on elucidating the protective mechanisms of ASP against IS-induced intestinal injury. We found that ASP can improve IS-induced intestinal injury by suppressing gut microbiota dysbiosis and the colonic LPS-TLR4-MAPK pathway, thereby inhibiting LPS leakage to the brain and attenuating brain injury. These findings suggest that APS mitigates IS-induced brain injury *via* modulating the microbiota-gut-brain axis.

5. Conclusion

Our findings reveal that ASP alleviates IS-induced brain injury by modulating the microbiota-gut-brain axis, as evidenced by integrated MCAO-induced animal models, ABX treatment, and FMT experiments (Fig. 9). The anti-ischemia effects of ASP are closely associated with its ability to modulate SCFA-producing bacteria, preserve intestinal barrier functions, inhibit LPS leakage, and microglial activation. Our study elucidates the mechanistic basis of ASP's therapeutic effects in IS and provides a theoretical foundation for developing ASP-based functional products from a neuroprotective perspective.

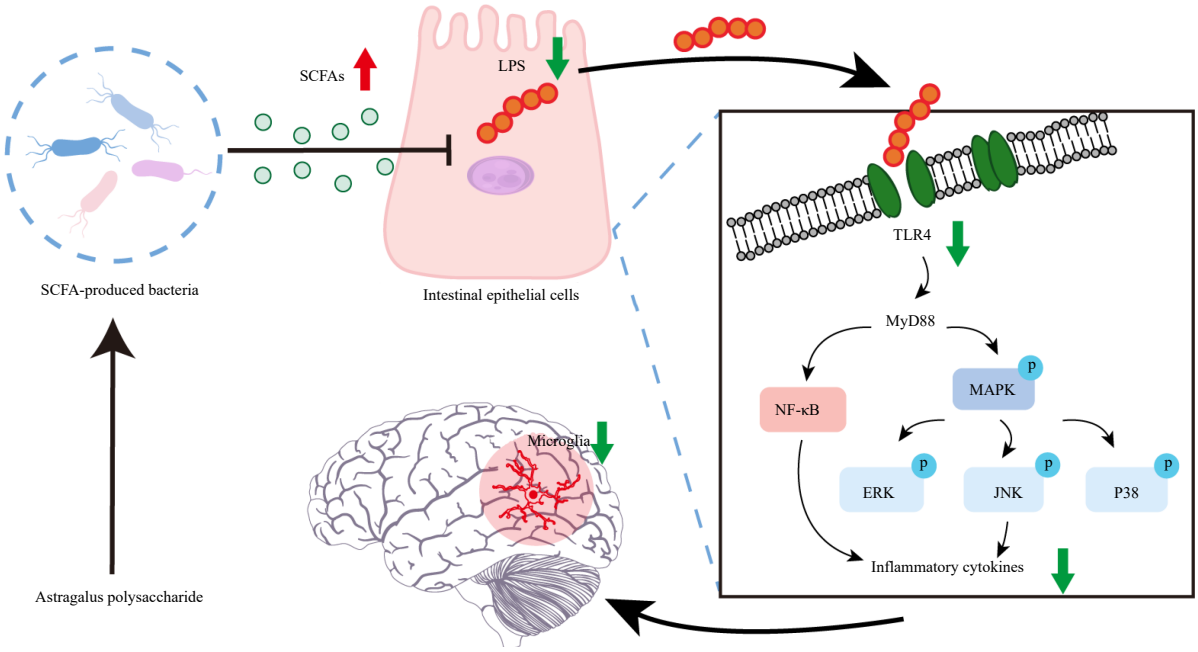


Fig. 9 Schematic diagram of ASP administration protects IS *via* the microbiota-gut-brain axis.

Funding

This work was supported by the National Natural Science Foundation of China (Nos. 82574737 and 82204973), Scientific and Technological Innovation Project of China Academy of Chinese Medical Sciences (Nos. CI2026A04906, CI2024E003, CI2021A00605 and CI2021B015), the Fundamental Research Funds for the Central Public Welfare Research Institutes of Institute of Chinese Materia Medica, China Academy of Chinese Medical Sciences (No. ZXKT25045 and ZXKT21030), the Special Program for Outstanding Young Scientific and Technological Talents (Innovation) of China Academy of Chinese Medical Sciences (No. ZZ15-YQ-034), and the Supportive Plan for Top Innovative PhD Students at China Academy of Chinese Medical Sciences.

Data availability

Data will be available on request by sending E-mail to the corresponding authors.

Declaration of competing interest

These authors have no conflict of interest to declare.

References

1 Walter K. What is acute ischemic stroke? *JAMA*. 2022;327:885. https://doi.org/10.1001/jama.2022.1420.
2 Yang RC, Yang B, Liu W, et al. Emerging role of non-coding RNAs in neuroinflammation mediated by microglia and astrocytes. *J Neuroinflammation*. 2023;20:173. https://doi.org/10.1186/s12974-023-02856-0.
3 Wang J, Zhang JH, Ye YZ, et al. Peripheral organ injury after stroke. *Front Immunol*. 2022;13:901209. https://doi.org/10.3389/fimmu.2022.901209.
4 Xu KY, Gao XX, Xia GH, et al. Rapid gut dysbiosis induced by stroke exacerbates brain infarction in turn. *Gut*. 2021;70(8):1486-1494. https://doi.org/10.1136/gutjnl-2020-323263.
5 Mendelson SJ, Prabhakaran S. Diagnosis and management of transient ischemic attack and acute ischemic stroke: a review. *JAMA*. 2021;325:1088-1098. https://doi.org/10.1001/jama.2020.26867.
6 Robba C, Battaglini D, Samary CS, et al. Ischaemic stroke-induced distal organ damage: pathophysiology and new therapeutic strategies. *Intensive Care Med Exp*. 2020;8(Suppl 1):23. https://doi.org/10.1186/s40635-020-00305-3.
7 Lee J, d'Aigle J, Atadja L, et al. Gut microbiota-derived short-chain fatty acids promote poststroke recovery in aged mice. *Circ Res*. 2020;127:453-465. https://doi.org/10.1161/CIRCRESAHA.119.316448.
8 Xiao WP, Su JB, Gao XJ, et al. The microbiota-gut-brain axis participates in chronic cerebral hypoperfusion by disrupting the metabolism of short-chain fatty acids. *Microbiome*. 2022;10:62. https://doi.org/10.1186/s40168-022-01255-6.
9 Erny D, Hrabě de Angelis AL, Jaitin D, et al. Host microbiota constantly control maturation and function of microglia in the CNS. *Nat Neurosci*. 2015;18:965-977. https://doi.org/10.1038/nn.4030.

10 Wu CH, Wu CY, Peng LX, et al. Multi-omics approaches for the understanding of therapeutic mechanism for Huang-Qi-Long-Dan Granule against ischemic stroke. *Pharmacol Res*. 2024;205:107229. https://doi.org/10.1016/j.phrs.2024.107229.
11 Brierley DI, de Lartigue G. Reappraising the role of the vagus nerve in GLP-1-mediated regulation of eating. *Br J Pharmacol*. 2022;179:584-599. https://doi.org/10.1111/bph.15603.
12 Xu L, Xu XY, Hou XQ, et al. Adjuvant therapy with *Astragalus membranaceus* for post-stroke fatigue: a systematic review. *Metab Brain Dis*. 2020;35:83-93. https://doi.org/10.1007/s11011-019-00483-4.
13 Zhao P, Su GH, Xiao XY, et al. Chinese medicinal herb Radix Astragali suppresses cardiac contractile dysfunction and inflammation in a rat model of autoimmune myocarditis. *Toxicol Lett*. 2008;182:29-35. https://doi.org/10.1016/j.toxlet.2008.08.002.
14 Liu CH, Tsai CH, Li TC, et al. Effects of the traditional Chinese herb *Astragalus membranaceus* in patients with poststroke fatigue: a double-blind, randomized, controlled preliminary study. *J Ethnopharmacol*. 2016;194:954-962. https://doi.org/10.1016/j.jep.2016.10.058.
15 Du Y, Wan HT, Huang P, et al. A critical review of *Astragalus* polysaccharides: from therapeutic mechanisms to pharmaceutics. *Biomed Pharmacother*. 2022;147:112654. https://doi.org/10.1016/j.biopha.2022.112654.
16 Wang MY, Zhu WF, Guo YM, et al. *Astragalus* polysaccharide treatment relieves cerebral ischemia–reperfusion injury by promoting M2 polarization of microglia by enhancing *O*-GlcNAcylation. *Metab Brain Dis*. 2024;40:16. https://doi.org/10.1007/s11011-024-01420-w.
17 Xu SW, Wusiman A, Liu ZG, et al. pH-responsive *Astragalus* polysaccharides-loaded poly(lactic-co-glycolic acid) nanoparticles and their *in vitro* immunogenicity. *Int J Biol Macromol*. 2019;125:865-875. https://doi.org/10.1016/j.ijbiomac.2018.12.156.
18 Conlon MA, Topping DL. Dietary polysaccharides and polyphenols can promote health by influencing gut microbiota populations. *Food Funct*. 2016;7:1730. https://doi.org/10.1039/c6fo90009g.
19 Ma JY, Liu XJ, Zhao Y, et al. Th17/Treg balance is regulated during the suppression of experimental autoimmune encephalomyelitis treated by *Astragalus* polysaccharides *via* the microbiota-gut-brain axis. *Brain Res Bull*. 2025;220:111171. https://doi.org/10.1016/j.brainresbull.2024.111171.
20 Liu DY, Zhu YY, Hou ZM, et al. Polysaccharides from *Astragalus membranaceus* Bunge alleviate LPS-induced neuroinflammation in mice by modulating microbe-metabolite-brain axis and MAPK/NF-κB signaling pathway. *Int J Biol Macromol*. 2025;304(Pt 1):140885. https://doi.org/10.1016/j.ijbiomac.2025.140885.
21 Ying Y, Song LY, Pang WL, et al. *Astragalus* polysaccharide protects experimental colitis through an aryl hydrocarbon receptor-dependent autophagy mechanism. *Br J Pharmacol*. 2024;181(5):681-697. https://doi.org/10.1111/bph.16229.
22 Huang YC, Bai J, Shui JM, et al. Simultaneous determination of the monosaccharide types and their absolute configurations in polysaccharides based on UPLC-MS/MS. *Int J Biol Macromol*. 2025;295:139647. https://doi.org/10.1016/j.ijbiomac.2025.139647.
23 Zhang J, Li Y, Chang ML, et al. Naoxintong capsule attenuates heart damage after ischemic stroke *via* Nuclear factor-κB/Pyrin domain-containing protein 3/Caspase-1 signaling. *J Ethnopharmacol*. 2025;341:119240. https://doi.org/10.1016/j.jep.2024.119240.
24 Li Y, Zhang J, Lei YX, et al. Multi-omics approaches reveal the therapeutic mechanism of Naoxintong capsule against ischemic stroke. *J Ethnopharmacol*. 2025;343:119435. https://doi.org/10.1016/j.jep.2025.119435.
25 Wang HD, Zhang MS, Li J, et al. Gut microbiota is causally associated with poststroke cognitive impairment through lipopolysaccharide and butyrate. *J Neuroinflammation*. 2022;19:76. https://doi.org/10.1186/s12974-022-02435-9.
26 Abdullahi W, Tripathi D, Ronaldson PT. Blood-brain barrier dysfunction in ischemic stroke: targeting tight junctions and transporters for vascular protection. *Am J Physiol Cell Physiol*. 2018;315:C343-C356. https://doi.org/10.1152/ajpcell.00095.2018.
27 Liao S, Wu JN, Liu RM, et al. A novel compound DBZ ameliorates neuroinflammation in LPS-stimulated microglia and ischemic stroke rats: role of Akt(Ser473)/GSK3β(Ser9)-mediated Nrf2 activation. *Redox Biol*. 2020;36:101644. https://doi.org/10.1016/j.redox.2020.101644.
28 Singh V, Lee G, Son H, et al. Butyrate producers, "The Sentinel of Gut": their intestinal significance with and beyond butyrate, and prospective use as microbial therapeutics. *Front Microbiol*. 2022;13:1103836. https://doi.org/10.3389/fmicb.2022.1103836.
29 Dai WH, Cai DD, Zhou S, et al. Uncovering a causal connection between the *Lachnoclostridium* genus in fecal microbiota and non-alcoholic fatty liver disease: a two-sample Mendelian randomization analysis. *Front Microbiol*. 2023;14:1276790. https://doi.org/10.3389/fmicb.2023.1276790.
30 Lee PC, Wu CJ, Hung YW, et al. Gut microbiota and metabolites associate with outcomes of immune checkpoint inhibitor-treated unresectable hepatocellular carcinoma. *J Immunother Cancer*. 2022;10:e004779. https://doi.org/10.1136/jitc-2022-004779.
31 De Vos WM, Nguyen Trung M, Davids M, et al. Phytate metabolism is mediated by microbial cross-feeding in the gut microbiota. *Nat Microbiol*. 2024;9:1812-1827. https://doi.org/10.1038/s41564-024-01698-7.
32 Li W, Liu YC, Zheng XM, et al. Rewiring tryptophan metabolism *via* programmable probiotic integrated by dual-layered microcapsule protects against inflammatory bowel disease in mice. *ACS Nano*. 2024;18:35443-35464. https://doi.org/10.1021/acsnano.4c12801.
33 Yadav SK, Ito N, Mindur JE, et al. Fecal Lcn-2 level is a sensitive biological indicator for gut dysbiosis and intestinal inflammation in multiple sclerosis. *Front Immunol*. 2022;13:1015372. https://doi.org/10.3389/fimmu.2022.1015372.
34 Koh YC, Hsu HW, Ho PY, et al. Feruloylacetone and its analog demethoxyferuloylacetone mitigate obesity-related muscle atrophy and insulin resistance in mice. *J Agric Food Chem*. 2025;73:1231-1243. https://doi.org/10.1021/acs.jafc.4c07798.
35 Grund M, Choi SJ, Powell L, et al. Intranasal immunization with a Bucl8-based vaccine ameliorates bacterial burden and pathological inflammation, and promotes an IgG2a/b dominant response in an outbred mouse model of Burkholderia infection. *Front Immunol*. 2023;14:1177650. https://doi.org/10.3389/fimmu.2023.1177650.
36 Bao ZY, Zhang ZY, Zhou GY, et al. Novel mechanisms and therapeutic targets for ischemic stroke: a focus on gut microbiota. *Front Cell Neurosci*. 2022;16:871720. https://doi.org/10.3389/fncel.2022.871720.
37 Nyati KK, Masuda K, Zaman MM-U, et al. TLR4-induced NF-κB and MAPK signaling regulate the IL-6 mRNA stabilizing protein Arid5a. *Nucleic Acids Res*. 2017;45:2687-2703. https://doi.org/10.1093/nar/gkx064.
38 Haupt M, Gerner ST, Bähr M, et al. Neuroprotective strategies for ischemic stroke-future perspectives. *Int J Mol Sci*. 2023;24:4334. https://doi.org/10.3390/ijms24054334.
39 Liang H, Tao Sm, Wang Yy, et al. *Astragalus* polysaccharide: implication for intestinal barrier, anti-inflammation, and animal production. *Front Nutr*. 2024;11:1364739. https://doi.org/10.3389/fnut.2024.1364739.
40 Schneider MR, Dahlhoff M, Horst D, et al. A key role for E-cadherin in intestinal homeostasis and Paneth cell maturation. *PLoS One*. 2010;5:e14325. https://doi.org/10.1371/journal.pone.0014325.
41 Scalise AA, Kakogiannos N, Zanardi F, et al. The blood-brain and gut-vascular barriers: from the perspective of claudins. *Tissue Barriers*. 2021;9:1926190. https://doi.org/10.1080/21688370.2021.1926190.
42 Mao MJ, Cao XQ, Liang YH, et al. Neuroprotection of rhubarb extract against cerebral ischaemia-reperfusion injury *via* the gut-brain axis pathway. *Phytomedicine*. 2024;126:155254. https://doi.org/10.1016/j.phymed.2023.155254.
43 Ling Y, Gong TY, Zhang JM, et al. Gut microbiome signatures are biomarkers for cognitive impairment in patients with ischemic stroke. *Front Aging Neurosci*. 2020;12:511562. https://doi.org/10.3389/fnagi.2020.511562.
44 Zhang XT, Wang XY, Zhao H, et al. Imbalance of microbacterial diversity is associated with functional prognosis of stroke. *Neural Plast*. 2023;2023:6297653. https://doi.org/10.1155/2023/6297653.
45 Płóciennikowska A, Hromada-Judycka A, Borzęcka K, et al. Co-operation of TLR4 and raft proteins in LPS-induced pro-inflammatory signaling. *Cell Mol Life Sci*. 2015;72:557-581. https://doi.org/10.1007/s00018-014-1762-5.
46 Yang S, Li WJ, Bai XY, et al. Ginseng-derived nanoparticles alleviate inflammatory bowel disease *via* the TLR4/MAPK and p62/Nrf2/Keap1 pathways. *J Nanobiotechnol*. 2024;22:48. https://doi.org/10.1186/s12951-024-02313-x.
47 Chen HR, Chen CW, Kuo YM, et al. Monocytes promote acute neuroinflammation and become pathological microglia in neonatal hypoxic-ischemic brain injury. *Theranostics*. 2022;12:512-529. https://doi.org/10.7150/thno.64033.
48 Stanley D, Mason LJ, Mackin KE, et al. Translocation and dissemination of commensal bacteria in post-stroke infection. *Nat Med*. 2016;22:1277-1284. https://doi.org/10.1038/nm.4194.
49 Yuan YK, Ma MJ, Zhang SZ. Recent advances in delivery systems of fucoxanthin. *Food Chem*. 2023;404(Pt B):134685. https://doi.org/10.1016/j.foodchem.2022.134685.
50 Ouyang J, Wang F, Li WJ, et al. Structure characterization of polysaccharide from Chinese Yam (*Dioscorea opposite* Thunb.) and its growth-promoting effects on *Streptococcus thermophilus*. *Foods*. 2021;10:2698. https://doi.org/10.3390/foods10112698.
51 Cai Y, Si ZY, Jiang Y, et al. Structure-activity relationship of low molecular weight *Astragalus membranaceus* polysaccharides produced by *Bacteroides*. *Carbohydr Polym*. 2023;316:121036. https://doi.org/10.1016/j.carbpol.2023.121036.
52 Tang LT, Xie SY, Wang DY, et al. *Astragalus* polysaccharide/carboxymethyl chitosan/sodium alginate based electroconductive hydrogels for diabetic wound healing and muscle function assessment. *Carbohydr Polym*. 2025;350:123058. https://doi.org/10.1016/j.carbpol.2024.123058.
53 Liao JZ, Li CY, Huang J, et al. Structure characterization of honey-processed *Astragalus* polysaccharides and its anti-inflammatory activity *in vitro*. *Molecules*. 2018;23:168. https://doi.org/10.3390/molecules23010168.
54 Chen GM, Jiang N, Zheng JP, et al. Structural characterization and anti-inflammatory activity of polysaccharides from *Astragalus membranaceus*. *Int J Biol Macromol*. 2023;241:124386. https://doi.org/10.1016/j.ijbiomac.2023.124386.
55 Lim JD, Yu CY, Kim SH. Structural characterization of an intestinal immune system-modulating arabino-3,6-galactan-like polysaccharide from the above-ground part of *Astragalus membranaceus* (Bunge). *Carbohydr Polym*. 2016;136:1265-1272. https://doi.org/10.1016/j.carbpol.2015.10.029.